International Journal of Pharmaceutics 541 (2018) 11–18

Contents lists available at ScienceDirect

International Journal of Pharmaceutics

journal homepage: www.elsevier.com/locate/ijpharm

Protective effect of sodium stearate on the moisture-induced deterioration of hygroscopic spray-dried powders

Jiaqi Yu[a], Maria-Cristina Romeo[a], Alex A. Cavallaro[b], Hak-Kim Chan[a,*]

[a] Advanced Drug Delivery Group, Faculty of Pharmacy, The University of Sydney, New South Wales 2006, Australia
[b] Future Industries Institute, University of South Australia, 5095, Australia

ARTICLE INFO

Keywords:
Dry powder inhaler (DPI)
Moisture protection
Aerosol performance
Spray drying
Excipients

ABSTRACT

Amorphous powders are thermodynamically unstable, significantly impacting the processing, storage and performance of a product. Therefore, stabilization of the amorphous contents is in demand. In this study, disodium cromoglycate (DSCG) powder was chosen as a model drug because it is amorphous and highly hygroscopic after spray drying. Sodium stearate (NaSt) was co-spray dried with DSCG at various concentrations (10, 50 and 90% w/w) to investigate its effect against moisture-induced deterioration on the *in vitro* aerosolization performance of DSCG. Particle size distribution and morphology were measured by laser diffraction and scanning electron microscopy (SEM). Physicochemical properties of the powders were analysed by X-ray powder diffraction (XRPD) and dynamic vapour sorption (DVS). Particle surface chemistry was analysed by the time-of-flight secondary ion mass spectrometry (ToF-SIMS). *In vitro* dissolution behaviours of the spray-dried (SD) powders were tested by the Franz cell apparatus. *In vitro* aerosolization performance of SD formulations stored at different relative humidity (RH) was evaluated by a multi-stage liquid impinger (MSLI), using an Osmohaler® at 100 L/min. Results showed that adding NaSt in the formulation not only increased the aerosolization performance of DSCG significantly, but also effectively reduced the deleterious impact of moisture. No significant difference was found in the fine particle fraction (FPF) of formulations containing NaSt before and after storage at both 60% and 75% RH for one week. However, after one month storage at 75% RH, SD formulation containing 10% NaSt showed a reduction in FPF, while formulations containing 50% or 90% NaSt showed no change. The underlying mechanism was that NaSt increased the crystallinity of the powders and its presence on the particle surface reduced particle aggregations and cohesiveness. However, NaSt at high concentration could reduce dissolution rate, which needs to be taken into consideration.

1. Introduction

Amorphous or partially amorphous pharmaceuticals are of interest for drug delivery to the lungs (Weers and Miller, 2015; Chen et al., 2016). The amorphous content in the pharmaceutical powders can be unwantedly produced or intentionally designed (Burnett et al., 2004; Yu et al., 2017). Regardless, amorphousness plays an important role in solid pharmaceutical systems, directly affecting the powder processing, storage and delivery (Burnett et al., 2004). In particular, stability related issues during powder processing and storage are a major concern as even a small amount of amorphous material could absorb relatively large amounts of moisture, significantly impacting the long-term stability and performances.

Spray drying is one primarily used technique for inhalable dry powder production, while often leaving the powders amorphous and physically unstable (Vehring, 2008). Subsequently, particle agglomerates may occur when the amorphous content absorbed moisture upon exposure to humidity (Zhou et al., 2016), causing adverse effects on the aerosol generation and lung deposition. One potential strategy for the prevention of moisture-induced deterioration in aerosolization performance is by coating moisture protective materials on the particle surface (Raula et al., 2008). Zhou et al. reported that SD colistin powders showed 30% decrease in FPF after storage at 75% RH for 24 h. However, no deterioration in FPF at the same storage condition was observed by co-spray drying with azithromycin at 1:1 mass ratio (Zhou et al., 2016). The protection was attributed to the occupying of azithromycin (96.5% molar fraction) on the co-SD particle surface (Zhou et al., 2016). Li et al. found that compared with SD DSCG powder, co-SD formulations containing 10–20% w/w L-leucine could achieve 61–73% (molar percent) coverage on the particle surface, and reduced the moisture-induced deterioration of DSCG after storage at 75% RH for 24 h but not after 4 weeks (Li et al., 2016). In our recent

* Corresponding author.
E-mail address: kim.chan@sydney.edu.au (H.-K. Chan).

https://doi.org/10.1016/j.ijpharm.2018.02.018
Received 19 January 2018; Received in revised form 13 February 2018; Accepted 15 February 2018
Available online 15 February 2018

study, three hydrophobic amino acids, isoleucine, valine and methionine, significantly reduced the deleterious effect of moisture on aerosol performance of DSCG, and the mechanism of the moisture protection was also related to the coverage of the amino acids on the particle surface (Yu et al., 2017).

Excipients were widely used in inhaled dry powder formulations in literature, but only a few have been approved by the FDA, including lactose monohydrate, 1,2-Distearoyl-*sn*-glycero-3-phosphocholine (DSPC), Calcium chloride ($CaCl_2$), gelatin, sulfuric acid, magnesium stearate (MgSt), titanium dioxide (TiO_2) and mannitol (FDA, 2017). MgSt is a well-known excipient which can be obtained from animals and vegetables, and it has been widely used as a lubricant in solid dosage form (Shur et al., 2016). Low moisture sorption behaviour was observed for MgSt under the RH exposure up to 90% (Swaminathan and Kildsig, 2001). Previous studies by Zhou et al. showed that 2% w/w MgSt had a substantial improvement in the aerosolization behaviour the micronized salbutamol sulphate powder after mechanofusion (Zhou et al., 2013). MgSt was reported to protect the drug from moisture and to reduce cohesion and adhesion between particles (Young et al., 2002; Lau et al., 2017). MgSt, however, is almost completely insoluble in water or most organic solvent system, often being used via mechanical approaches (Kumon et al., 2008; Zhou et al., 2010, 2011a,b, 2013). Compared with MgSt, NaSt is more soluble in water or co-solvent system (Supplementary materials), being more potential to be used as a surface coating material via spray drying (Parlati et al., 2009). Thus, NaSt was chosen as an excipient in this study to investigate its effect on the moisture protection of hygroscopic SD DSCG powders.

2. Materials and methods

2.1. Materials

DSCG was purchased from Zhejiang Esun Chemical Co., Ltd. (Hangzhou, China) and sodium stearate was sourced from ACROS Organics (New Jersey, USA). Phosphate buffered saline (PBS) and L-ascorbic acid were purchased from Sigma-Aldrich (Castle Hill, Australia). All the chemicals were of analytical grade except the HPLC grade methanol. Deionized water was from Modulab Type II Deionization System (Sydney, Australia). High purity compressed nitrogen gas (North Ryde, Australia) was used for spray drying. Commercial Osmohaler® inhaler was sourced from Pharmaxis Ltd. (Frenches Forest, Australia) and hydroxypropyl methylcellulose transparent size 3 capsules were from Capsugel (West Ryde, Australia).

2.2. Powder formulation

A feed solution (10 mg/ml total solutes) was prepared by dissolving NaSt and DSCG at a known mass ratio (10%, 50% and 90% mass ratio) in 50% ethanol using a 40 °C water bath. The drug solution was pumped into a B-290 lab scale spray-dryer (Büchi Falwil, Switzerland) connected to a B-295 inert loop (Büchi Falwil, Switzerland). High purity dry nitrogen was used as the atomizing gas. The spray-dryer was operated at the following conditions: feed rate of 1.8 mL/min, atomizer setting 742 L/h, aspirator of 35 m^3/h, inlet N_2 temperature 100 °C and outlet N_2 temperature 68–70 °C. After spray drying, all powders were stored in a desiccator containing silica gel at room temperature for further analysis.

2.3. Particle size

A Scirocco 2000 accessory dry powder dispersion unit (Malvern Instruments, UK) was applied for particle size distribution measurement of the SD powders, under an air pressure of 2.0 bar. D_{10}, D_{50}, and D_{90} (i.e. particle size under 10%, 50% and 90%, respectively) and span (i.e. difference between D_{10} and D_{90} divided by D_{50}) were calculated from the size distribution results. Each formulation was measured in triplicate.

2.4. Particle morphology

Powders from each formulation were spread on a stub and sputter coated with 15 nm thick gold using a Quorum Emitech K550X sputter coater (Kent, UK). A Carl Zeiss scanning electron microscopy (Oberkochen, Germany) at 3 kV was used for capturing SEM images of the particle morphology.

2.5. Crystallinity

Crystallinity of the powder was measured on a Shimadzu X-ray powder diffraction (XRPD) 6000 (Kyoto, Japan) with Cu-Kα radiation set at 40 kV and the current at 30 mA. The results were recorded from 5° to 50° by the 2θ method at a scan speed of 2° per minute.

2.6. Dynamic water vapour sorption

A dynamic vapour sorption system (DVS-1, Surface Management Systems, London, UK) was used for measuring the moisture sorption behaviour of the SD samples. 5–10 mg of powder was placed in the measurement chamber under a continuous N_2 gas flow at 25 °C. The RH inside the chamber was maintained in the range of 0–90%, with 10% increments or decrements for the sorption and desorption cycle, respectively. Moisture uptake was considered to have reached equilibration when the value of weight change dm/dt was smaller than 0.002% per minute.

2.7. Time-of-Flight secondary ion mass spectrometry

Time-of-Flight secondary ion mass spectrometry was conducted on a Physical Electronic TRIFT V nanoToF instrument (Physical Electronics Inc., Chanhassen, MN, USA) which was equipped with a pulsed liquid metal $^{79+}$Au primary ion gun (LMIG) under 30 keV energy operate in either “bunched” mode to optimize mass resolution and “unbunched” mode to optimize spatial resolution for imaging. Dual charge neutralization was provided by a 10 eV electron flood gun and 10 eV Ar + ions. All experiments were carried out under a vacuum of 5×10^{-6} Pa or lower. All data were collected and interpreted with WinCadenceN software (ULVAC-PHI Inc., Chanhassen, MN, USA). More detailed descriptions could be found in published works elsewhere (Zhou et al., 2011a,b, 2014; Li et al., 2016; Wang et al., 2016).

Pure DSCG and NaSt were analysed to identify their responses before the components were mapped in the co-SD formulations. The obtained data were then compared qualitatively by preparing plots of average normalized counts with 95% confidence intervals for each fragment of interest (Li et al., 2016). In this study, the mass spectra collected for DSCG and NaSt were analysed by the following dominants, characteristic responses: m/z ~181 ($C_3H_3O_2^+$) and ~229 atomic mass unit (amu) for DSCG, and m/z ~127 ($C_3H_5^+$) amu for NaSt.

2.8. Powder storage

Powders were stored separately in an open clean glass vial for each formulation in a humidity cabinet (Thermoline, Australia) at 60% RH or in a desiccator containing saturated sodium chloride solution (75 ± 5% RH), both at 25 °C for one week and one month.

2.9. In vitro aerosolization performance

A multi-stage liquid impinger (Copley, UK) connected to a USP throat with a silicone mouthpiece adapter (Westech Instrument, UK) was employed to analyse the *in vitro* aerosol performance of the SD powers before and after storage. 4 L of air was passed through the Osmohaler® (Pharmaxis Ltd., Australia) at a flowrate of 100 L/min for

2.4 s, at 4 kPa pressure drop across the device. The cut-off diameters of stages 1–4 at such flow rate are 10.4, 4.9, 2.4 and 1.2 μm, respectively. 10 ± 1 mg of powders were loaded in a size 3 capsule (Capsugel, Australia) and then dispersed through the Osmohaler® device in a controlled environment cabinet at 25 ± 2 °C and the targeted RH. Particles deposited on the capsule, inhaler, adapter, throat and stages would be rinsed carefully with deionized water and then collected for chemical assay. The glass filter was washed and sample was centrifuged at 13,400 rpm for 20 min (Westbury, USA) to obtain the supernatant. Dispersion for each formulation was carried out in triplicate.

2.10. In vitro dissolution profile of DSCG

A Franz cell dissolution system together with a heated stirring station (V6B, Perm Gear Inc., Bethlehem, U.S.A.) were applied to test the *in vitro* dissolution profiles of the four SD formulations. PBS (pH = 7.4) containing 2% ascorbic acid was used as dissolution medium and the liquid temperature was maintained at 37 °C throughout the experiment by a water bath. Further details of the method were described elsewhere (Chan et al., 2013; Parumasivam et al., 2016; Wang et al., 2016).

Powder samples (2.0–3.0 mg) deposited on a 0.45 μm cellulose filter paper were weighed accurately and the filter paper was then placed in between the buffer meniscus of the Franz cell. At predetermined time points within 3 h, approx. 550 μl of aliquot was withdrawn from the dissolution medium and replaced with the same amount of fresh buffer. After measurement, the filter membrane was removed and washed with 3 mL of fresh buffer solution. DSCG drug was quantified using a HPLC method described below. Each formulation was measured in triplicate.

2.11. Drug quantification

A high-performance liquid chromatography system (Shimadzu, Japan) and a Luna C18 column (μm, 250 × 4.60 mm; Phenomenex, USA) were applied to determine the concentration of DSCG (Li et al., 2016). The mobile phase consisted of 0.025 mol/L monobasic potassium phosphate (pH = 3.0) and methanol at 55:45 (v/v) ratio. UV detection wavelength was 326 nm, flow rate was 1.0 mL/min and injection volume was 20 μl. Fresh standards were prepared prior to each HPLC measurement.

Emitted dose fraction (ED, %) was defined as the total mass percentage of the drug particles collected from all parts except the capsule and inhaler device relative to the total recovered drug. Fine particle fraction (FPF, %) was defined as the total mass percentage of the drug particles with an aerodynamic diameter smaller than 4.9 μm (i.e., the total amount of drug particles collected from stage 2 and below) relative to the total recovered drug.

2.12. Statistical analysis

One-way analysis of variance (ANOVA) software was applied for testing statistical differences. The statistical differences were considered as significant if the probability values were < 0.05.

3. Results

3.1. Physicochemical properties

3.1.1. Particle size

Table 1 presented the particle size distribution results of the SD powder formulations. Most particles of each formulation had relatively narrow size distributions of < 5 μm and with spans in the range of 1.0–2.0, which were suitable for DPI formulation. Among all SD formulations, DSCG alone had a relative small D_{50} value of 1.07 ± 0.02 μm, and D_{50} values of co-SD formulations containing NaSt were around 1.5 μm.

Table 1
Particle size distribution of spray-dried powder formulations measured by laser diffraction. Mean ± SD, n = 3.

Formulation	D_{10} (μm)	D_{50} (μm)	D_{90} (μm)	Span
DSCG	0.46 ± 0.02	1.07 ± 0.02	2.50 ± 0.04	1.91 ± 0.09
10% NaSt + 90% DSCG	0.64 ± 0.01	1.55 ± 0.01	3.57 ± 0.04	1.89 ± 0.04
50% NaSt + 50% DSCG	0.66 ± 0.01	1.52 ± 0.01	3.39 ± 0.20	1.72 ± 0.01
90% NaSt + 10% DSCG	0.71 ± 0.01	1.53 ± 0.01	3.57 ± 0.02	1.56 ± 0.01

3.1.2. Particle morphology

Results of particle size observed by SEM observation (Figs. 1 and 2) and measured by laser diffraction were in good agreement. Fig. 1(a–c) showed the morphology of SD DSCG powder particles stored under different conditions. Similar to our previous study (Yu et al., 2017), the morphology of SD DSCG particles (Fig. 1a) was near-spherical with rough surfaces. After storage at 60% (Fig. 1b) and 75% RH (Fig. 1c) for one week, the particles fused into solid aggregates. Fig. 2(A–C)-1 showed the powder morphology of co-SD formulations containing NaSt. Overall, increasing the amount of NaSt resulted in particles with corrugated surfaces. After storage at 60% and 75% RH for one week, the surface morphology of particles in these formulations remained unchanged, being unaffected by the moisture. While after being stored at 75% RH for one month, the SD DSCG particles (Fig. 3a) became irregular and collapsed, which were similar to our previous study (Yu et al., 2017). In contrast, particle morphology of the co-SD formulations containing NaSt was maintained (Fig. 3b–d).

3.1.3. Crystallinity

A broad peak was shown at 25° in the XRPD diffractogram (Fig. 4a) of SD DSCG powders, suggesting the amorphous state. In contrast, SD NaSt showed distinct peaks (e.g. at 7°, 12°, 20° and 24°), confirming the crystalline form. For co-SD formulations containing NaSt, the intensities of peaks were related to the ratio of two components. Overall, increasing the amount of NaSt resulted in more distinguishable crystalline peaks compared with SD DSCG particles. After one month storage at 75% RH, the XRPD diffractogram of the SD powders (Fig. 4b) changed, with the occurrence of small crystalline peaks at different angles (10°, 25° and 28°). The XRPD patterns of formulations containing 50% and 90% NaSt were less affected compared with the formulation containing 10% NaSt, which may be related to their aerosol performances against moisture (in later discussion).

3.1.4. Water sorption

SD pure DSCG powders underwent a significant mass increase (up to 50%) at the dynamic water sorption cycle ranging from 0 to 90% RH (Fig. 5a), which was similar to our previous study (Yu et al., 2017). In contrast, SD pure NaSt absorbed about 3% at the elevated RH. With increasing amount of NaSt in the formulations, moisture uptake at the elevated RH was decreased. Interestingly, the water uptake and the percentage of DSCG showed a linear relationship at certain RHs (Fig. 5b), suggesting that in the co-SD formulations, NaSt had little effect on the water uptake by DSCG. For the co-SD powders, all formulations exhibited a similar reversible moisture sorption trend with no moisture induced recrystallization. All tested formulations showed a desorption hysteresis behaviour as the water molecules escaped slower during desorption cycle (Zhu et al., 2008).

3.1.5. Distribution of NaSt on the particle surface

As the peaks correlating to the larger ion fragments were of low intensity, characteristic smaller mass fragments with higher intensity were used to visualize the distribution of NaSt and DSCG on the surface of the samples. Fig. 6(a–e) shows the overlay of the chemical

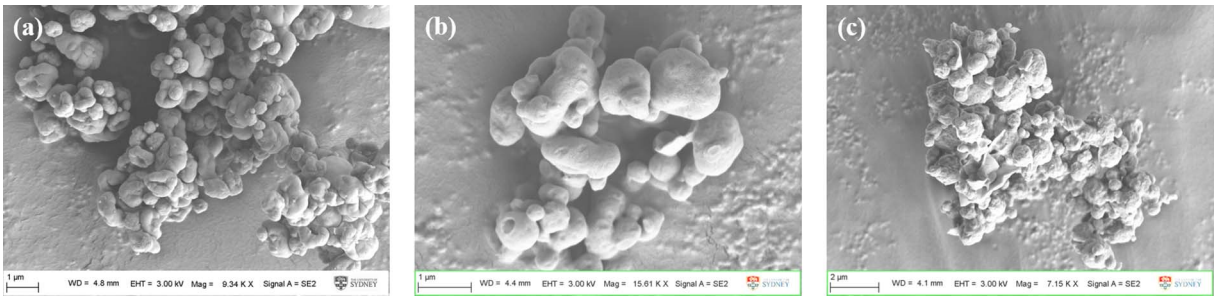

Fig. 1. SEM micrographs of SD DSCG alone powder at different conditions: (a) Desiccator; (b) 60% RH one week; (c) 75% RH one week.

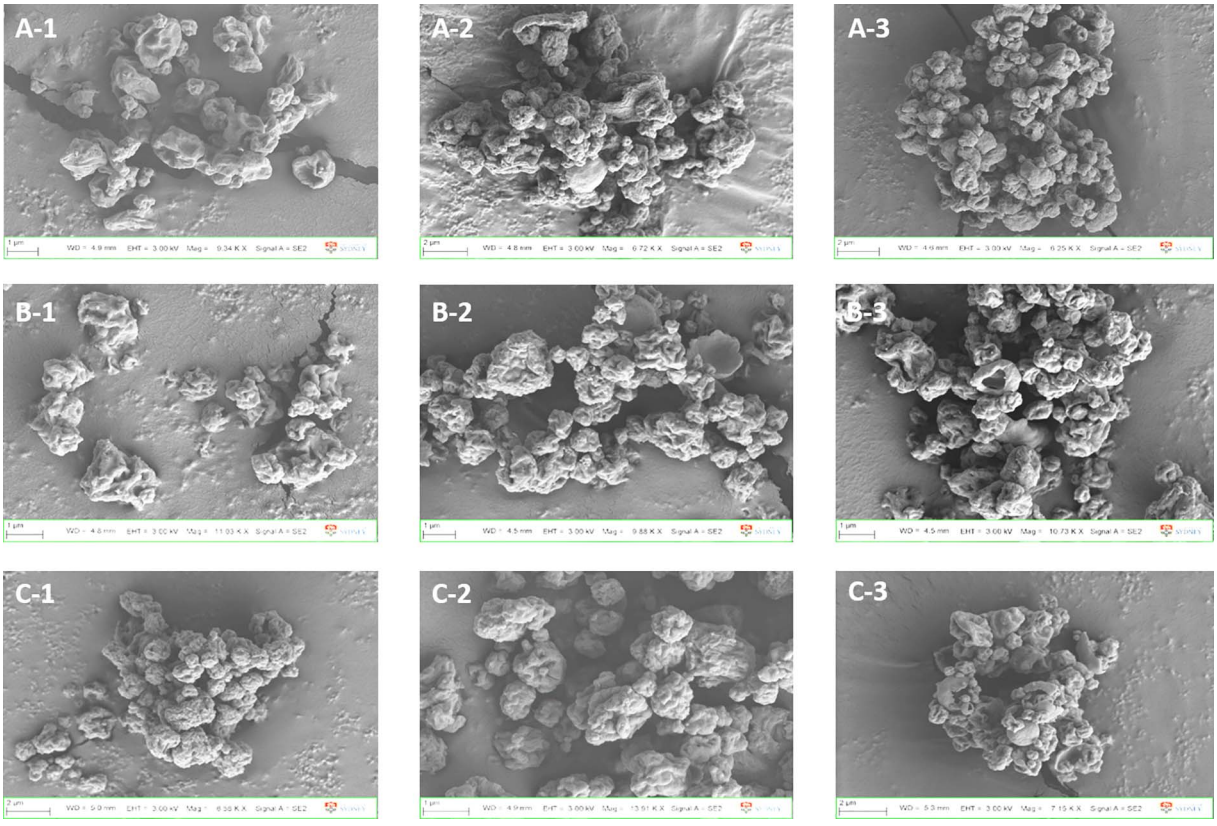

Fig. 2. SEM micrographs of SD powder formulations containing NaSt and DSCG at different ratios: (A) SD 10% NaSt + 90% DSCG; (B) SD 50% NaSt + 50% DSCG; (C) SD 90% NaSt + 10% DSCG; 1-Desiccator; 2–60% RH one week; 3–75% RH one week.

distribution of $C_3H_5^+$ (green) and $C_3H_3O_2^+$ (red) from NaSt and DSCG, respectively, as imaged via ToF-SIMS. ToF-SIMS probes the chemical composition at an average depth of 1–2 nm. The overlay images of $C_3H_5^+$ and $C_3H_3O_2^+$ demonstrate the change of surface composition towards complete NaSt surface coverage with increasing concentration ratio in the formulation.

The relative amount of DSCG and NaSt on the particle surface is difficult to quantify due to the similarity in elemental composition between the two compounds. However, it was observed that the normalized intensity of DSCG specific mass fragment (at m/z ~229 amu) peaks showed a decreasing trend with the increase of NaSt in the formulation (Fig. 7). The presence of this fragment in the 10% NaSt sample revealed an incomplete surface overage by the NaSt. As the concentration of NaSt is increased to 50% and 90%, DSCG associated peaks decrease to levels comparable to the NaSt control. This suggests that the outermost surface of these formulations entirely consists of NaSt.

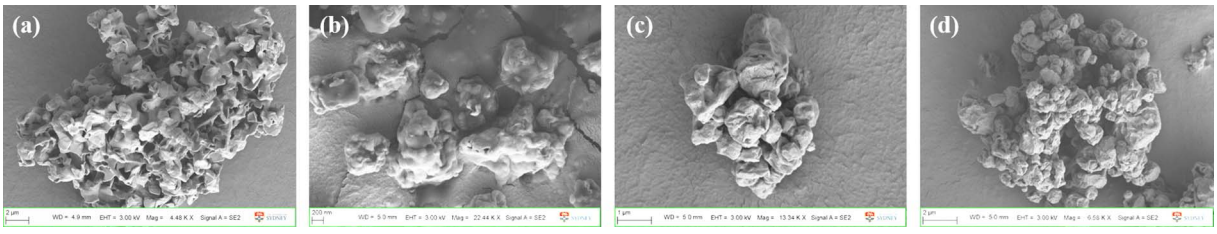

Fig. 3. SEM micrographs of SD powder formulations containing NaSt and DSCG at different ratios under 75% RH for one month: (a) SD DSCG; (b) SD 10% NaSt + 90% DSCG; (c) SD 50% NaSt + 50% DSCG; (d) SD 90% NaSt + 10% DSCG.

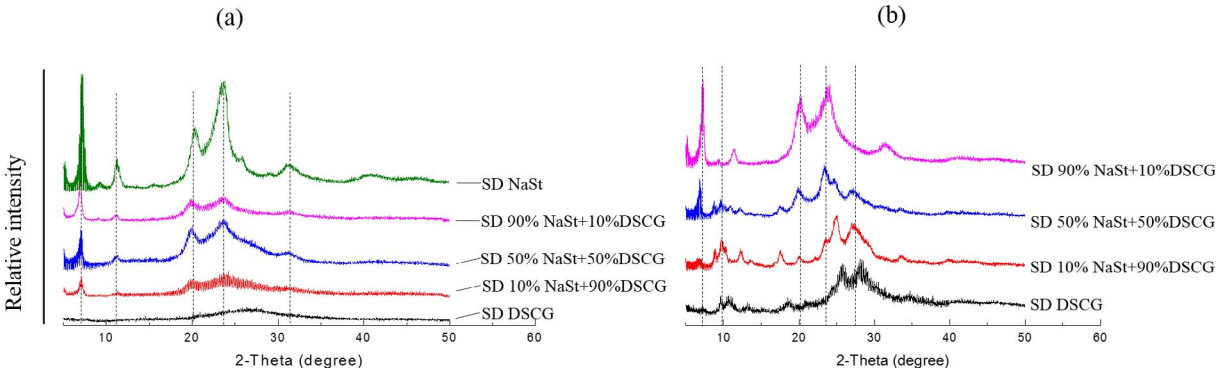

Fig. 4. X-ray powder diffraction patterns of SD powder formulations, (a) desiccator (b) 75% RH, one month.

3.2. In vitro aerosolization performance

Fig. 8(a–d, desiccator) showed the aerosolization performance of SD powders. All spray-dried formulations had a high emitted dose of > 85%. There was no significant difference in the emitted dose ($p > 0.05$) among formulations. The FPF and ED for SD DSCG alone were 68.1 ± 4.8% and 85.4 ± 5.8%, respectively. The dispersion results showed that co-SD formulations had a significantly higher FPF ($p < 0.05$) compared with SD DSCG alone, via a reduction of particle retention in the capsule and significant deposition increases in the impactor stage 4 and filter stage ($p < 0.05$). For co-SD powders containing 10% w/w NaSt, the ED and FPF were increased to 88.5 ± 0.6% and 85.5 ± 1.0%, respectively. Interestingly, formulations with higher amounts of NaSt (50% and 90%) did not show further improvement in the aerosol performance of the DSCG.

3.3. Effect of humidity on aerosolization

Fig. 8 also presented the aerosol performance of SD formulations after one week and one month of storage at 60% and 75% RH, respectively. The FPF of SD DSCG alone powder fell dramatically to 39.6 ± 3.3% at 60% RH and 6.3 ± 1.17% at 75% RH, respectively (Fig. 8a). In contrast, the presence of NaSt significantly reduced the effects of moisture on the aerosol performance of DSCG. There is no

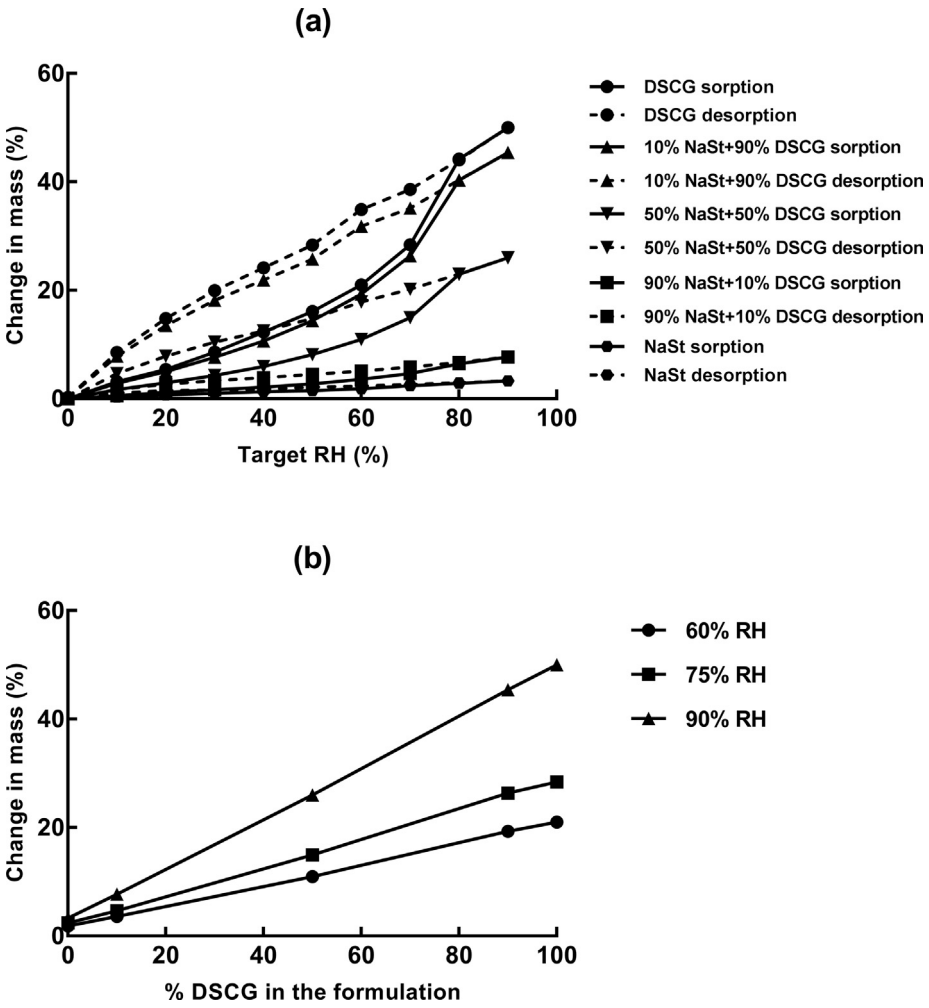

Fig. 5. (a) Dynamic water sorption behaviour of SD powder formulations; (b) relationships between the percent of DSCG in the formulations and water uptake at different RHs.

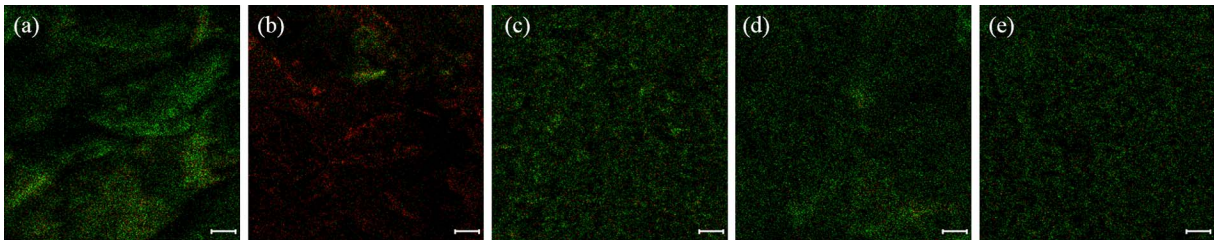

Fig. 6. Overlay mapping of $C_3H_5^+$ (green) and $C_3H_3O_2^+$ (red) on the surface of particles measured by ToF-SIMS (scale bar represents 10 μm): (a) NaSt; (b) DSCG; (c) SD 10% NaSt + 90% DSCG; (d) SD 50% NaSt + 50% DSCG; (e) SD 90% NaSt + 10% DSCG. (For interpretation of the references to colour in this figure legend, the reader is referred to the web version of this article.)

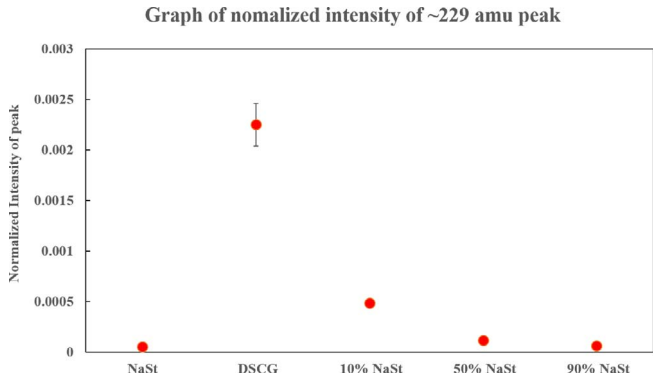

Fig. 7. Graph of normalized intensity of the DSCG specific mass fragment at *m/z* ~ 229 amu.

significant difference in the FPF ($p > 0.05$) of co-SD powders containing 10%, 50% and 90% NaSt before and after storage at both 60% and 75% RH for one week. However, after storage at 75% RH for one month, SD '10% NaSt + 90% DSCG' showed a significant decrease in FPF (74.7 ± 3.3%, $p < 0.05$). In contrast, formulations containing 50% or 90% NaSt maintained the FPF ($p > 0.05$) of the DSCG (84.3 ± 2.0% and 86.8 ± 1.7%, respectively) under the same storage condition. Interestingly, SD '10% NaSt + 90% DSCG' could maintain the FPF (85.8 ± 0.8%) after being stored at 60% RH for one month (in Supplementary materials).

3.4. In vitro dissolution profiles of DSCG

Fig. 9 showed the *in vitro* dissolution results of DSCG from the Franz cell measurement. SD DSCG and SD 10% NaSt + 90% DSCG had similar rapid dissolution profiles, where about 60% of total drug dissolved in the first 15 min. Formulations containing 50% and 90% NaSt had a slower dissolution rate, with approximately 40% and 20% of drug dissolved in the first 15 min, respectively. The maximum drug dissolved

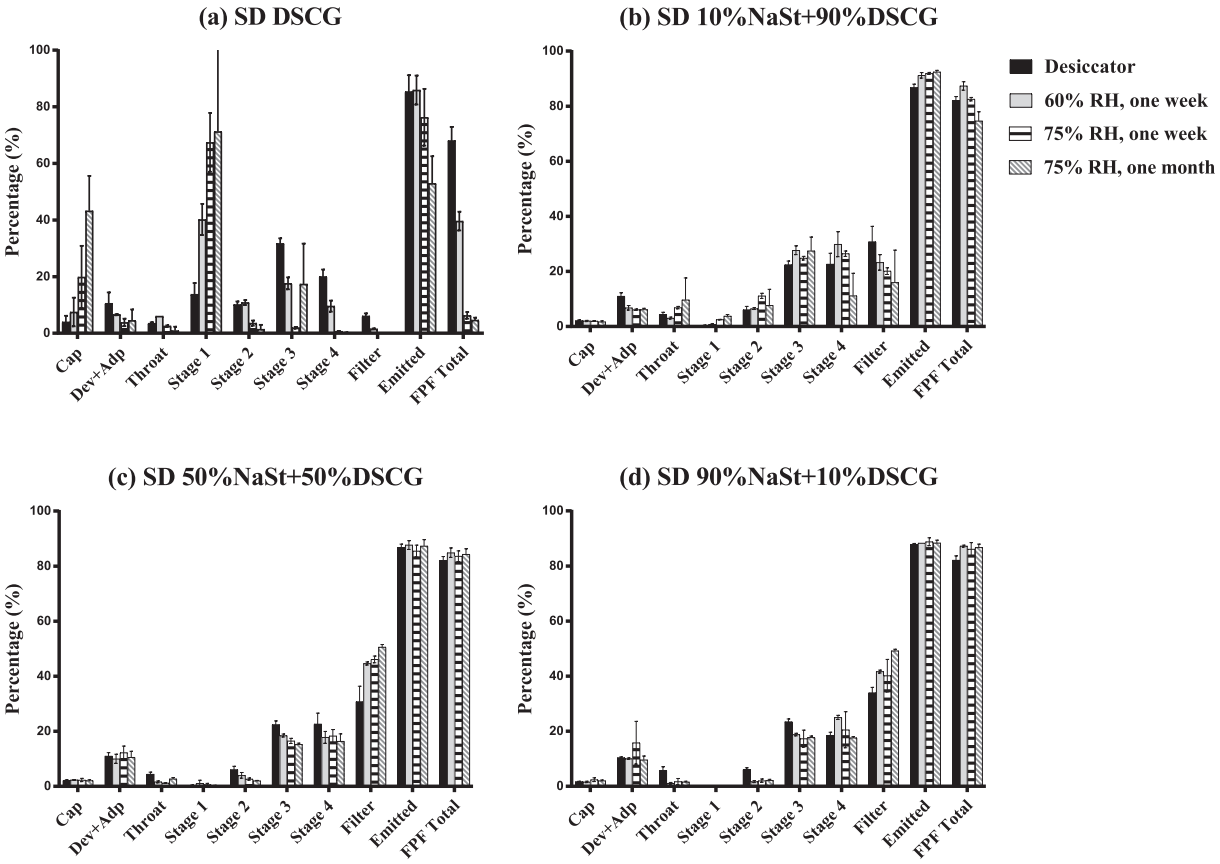

Fig. 8. The effect of moisture on *in vitro* aerosolization performances of SD NaSt/DSCG powders: (a) SD DSCG, (b) SD 10% NaSt + 90% DSCG, (c) SD 50% NaSt + 50% DSCG, and (d) SD 90% NaSt + 10% DSCG.

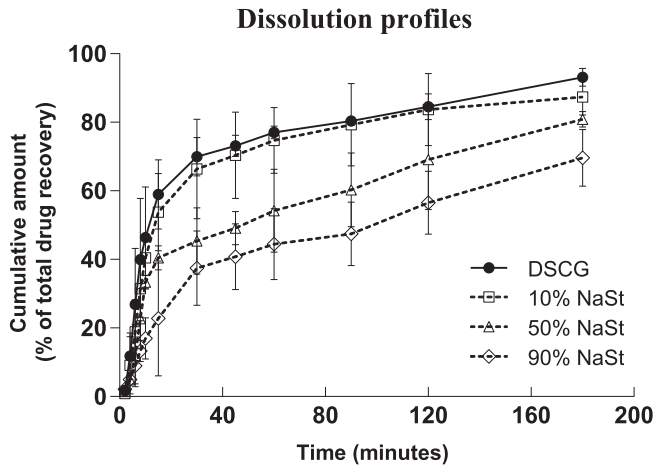

Fig. 9. Dissolution profiles of DSCG from SD formulations.

in 3 h for SD DSCG and SD 10% NaSt + 90% DSCG powders was about 90%, which was reduced by approx. 15% and 25% in formulations containing 50% and 90% NaSt, respectively.

4. Discussion

The hygroscopic nature of the SD powders is a challenge since moisture uptake can result in both physical and chemical instabilities of solid dosage forms (Li et al., 2016). DSCG powders after spray drying were amorphous and underwent a significant mass increase of 50% from water absorption at 90% RH. After storage at 75% RH for one week, the FPF of SD DSCG particles fell dramatically and became not inhalable. In the current study, we found that NaSt had a positive effect on improving the aerosolization performance as well as protecting DSCG against moisture. Results showed that formulation containing 10% NaSt preserved the FPF at elevated (60% and 75%) RH storage conditions for one week, but failed at 75% RH storage for one month. However, when the content of NaSt was increased to 50% and 90%, the co-SD formulations maintained the FPF even after storage at 75% RH for one month. In addition, formulations containing 50% and 90% NaSt showed a slower *in vitro* dissolution rate of DSCG, due to coating of the particles by NaSt which is less water soluble than DSCG (see below). Although the '10% NaSt' formulation showed a 45% mass increase at 90% RH, the existence of NaSt in the formulation showed a significant difference in protection against moisture-induced deterioration compared with SD DSCG powder alone. The moisture protective mechanism was probably attributed to the enrichment of NaSt on the particle surface, reducing particle-particle and particle-moisture interactions, thus facilitating dispersions. When two or more components were dried together in a droplet, redistribution on the particle surface can be driven by the difference in diffusivity, solubility, density, surface activity and hydrophobicity of each component (Porowska et al., 2016). In this study, the molecular weight of DSCG and NaSt is 512.3 and 306.5 g/mol, respectively, suggesting that they would have similar diffusion rate when dried in a droplet and thus could be evenly distributed throughout the drying solid. However, NaSt has a much lower aqueous solubility than DSCG (Index, 1968) and is a surface active (Tay et al., 2012). Therefore, this hydrophobic excipient would accumulate at the droplet liquid-gas interface during drying and deposits on the dried particles surface (Parlati et al., 2009), as seen in the Tof-SIMS images (Fig. 6). The early formulation of a NaSt-enriched shell could have prevented further shrinkage of the particles, resulting in slightly larger particle size for the co-SD formulations (Table 1). The accumulated NaSt on the surface would result in a large reduction in interfacial tension between the contiguous microparticles (Parlati et al., 2009), leading to a significant improvement of the aerosolization efficiency as well as moisture protection for the dry powder formulations. Another factor that contributed to the moisture protection is likely the crystallinity of NaSt, as materials in the crystalline state will typically have less water vapour sorption than the amorphous state due to the reduction in free energy, void space and/or surface area (Burnett et al., 2004). As shown in the XRPD (Fig. 4a), formulations containing 50% or 90% NaSt showed higher intensities of crystalline peaks compared with the formulation containing 10% NaSt. More interestingly, we found that after one month storage at 75% RH, there were less changes in the XRPD patterns of powders containing 50% and 90% NaSt compared with those containing 10% NaSt (Fig. 4b), which was also consistent with the aerosolization performances against moisture. During the drying process, NaSt was expected to reach supersaturation early in the process and crystallized out (Sadd et al., 1992). The presence of non-hygroscopic crystalline NaSt on the particle surface reduced the potential of interactions between particle surface and moisture (Li et al., 2016), thereby reducing the water uptake (Fig. 5a). However, after being stored at 75% RH for one month, SD '10% NaSt + 90% DSCG' showed a significant decrease in FPF, which is likely due to the incomplete surface coverage of NaSt. We have also investigated formulations containing 0.1% and 1.0% NaSt and found their aerosol performances deteriorated dramatically after one week storage at 75% RH similar to the SD DSCG powder (Supplementary materials), further supporting the moisture protection offered by NaSt is concentration dependent.

5. Conclusions

The addition of NaSt in inhalable powder formulations not only improved the *in vitro* aerosol performance, but also decreased moisture-induced deterioration in aerosolization. The proposed mechanism for this enhancement is the crystallinity and coverage of NaSt on the particle surface. This in turn is dependent on the concentration of NaSt present in the formulation. This investigation broadens the current understanding on sodium stearate as a moisture protective excipient on hygroscopic powders for inhalation drug delivery.

Acknowledgements

This work was supported by Australian Research Council's *Discovery Projects* funding scheme (ARC, DP 160102577). H-KC thanks Richard Stenlake for his generous donation which was used as part of a University of Sydney PhD scholarship to financially support JY. The authors acknowledge the facilities, and the scientific and technical assistance of the Australian Microscopy & Microanalysis Research Facility at both the University of Sydney and the University of South Australia.

Appendix A. Supplementary data

Supplementary data associated with this article can be found, in the online version, at http://dx.doi.org/10.1016/j.ijpharm.2018.02.018.

References

Burnett, D., Thielmann, F., Booth, J., 2004. Determining the critical relative humidity for moisture-induced phase transitions. Int. J. Pharm. 287 (1), 123–133.
Chan, J.G.Y., Chan, H.-K., Prestidge, C.A., Denman, J.A., Young, P.M., Traini, D., 2013. A novel dry powder inhalable formulation incorporating three first-line anti-tubercular antibiotics. Eur. J. Pharm. Biopharm. 83 (2), 285–292.
Chen, L., Okuda, T., Lu, X.-Y., Chan, H.-K., 2016. Amorphous powders for inhalation drug delivery. Adv. Drug Deliv. Rev. 100, 102–115.
(FDA), U. S. F. D. A., 2017. Inactive Ingredients Database. From: < https://www.fda.gov/Drugs/InformationOnDrugs/ucm113978.htm > .
Index, M., 1968. The Merck index: an encyclopedia of chemicals and drugs. Merck & Co 1406, 726.
Kumon, M., Machida, S., Suzuki, M., Kusai, A., Yonemochi, E., Terada, K., 2008. Application and mechanism of inhalation profile improvement of DPI formulations by mechanofusion with magnesium stearate. Chem. Pharm. Bull. 56 (5), 617–625.
Lau, M., Young, P.M., Traini, D., 2017. Co-milled API-lactose systems for inhalation

therapy: impact of magnesium stearate on physico-chemical stability and aerosolization performance. Drug Dev. Ind. Pharm. 43 (6), 980–988.
Li, L., Sun, S., Parumasivam, T., Denman, J.A., Gengenbach, T., Tang, P., Mao, S., Chan, H.-K., 2016. L-Leucine as an excipient against moisture on in vitro aerosolization performances of highly hygroscopic spray-dried powders. Eur. J. Pharm. Biopharm. 102, 132–141.
Parlati, C., Colombo, P., Buttini, F., Young, P.M., Adi, H., Ammit, A.J., Traini, D., 2009. Pulmonary spray dried powders of tobramycin containing sodium stearate to improve aerosolization efficiency. Pharm. Res. 26 (5), 1084–1092.
Parumasivam, T., Chan, J., Pang, A., Quan, D., Triccas, J., Britton, W., Chan, H., 2016. In vitro evaluation of inhalable verapamil-rifapentine particles for tuberculosis therapy. Mol. Pharm. 13 (3), 979–989.
Porowska, A., Dosta, M., Fries, L., Gianfrancesco, A., Heinrich, S., Palzer, S., 2016. Predicting the surface composition of a spray-dried particle by modelling component reorganization in a drying droplet. Chem. Eng. Res. Des. 110, 131–140.
Raula, J., Thielmann, F., Kansikas, J., Hietala, S., Annala, M., Seppälä, J., Lähde, A., Kauppinen, E.I., 2008. Investigations on the humidity-induced transformations of salbutamol sulphate particles coated with L-leucine. Pharm. Res. 25 (10), 2250–2261.
Sadd, P., Lamb, J., Clift, R., 1992. The effect of surfactants on heat and mass transfer to water drops in air. Chem. Eng. Sci. 47 (17–18), 4415–4424.
Shur, J., Price, R., Lewis, D., Young, P.M., Woollam, G., Singh, D., Edge, S., 2016. From single excipients to dual excipient platforms in dry powder inhaler products. Int. J. Pharm. 514 (2), 374–383.
Swaminathan, V., Kildsig, D.O., 2001. An examination of the moisture sorption characteristics of commercial magnesium stearate. AAPS PharmSciTech 2 (4), 73–79.
Tay, T., Morton, D.A., Gengenbach, T.R., Stewart, P.J., 2012. Dissolution of a poorly water-soluble drug dry coated with magnesium and sodium stearate. Eur. J. Pharm. Biopharm. 80 (2), 443–452.
Vehring, R., 2008. Pharmaceutical particle engineering via spray drying. Pharm. Res. 25 (5), 999–1022.
Wang, W., Zhou, Q.T., Sun, S.-P., Denman, J.A., Gengenbach, T.R., Barraud, N., Rice, S.A., Li, J., Yang, M., Chan, H.-K., 2016. Effects of surface composition on the aerosolisation and dissolution of inhaled antibiotic combination powders consisting of colistin and rifampicin. AAPS J. 18 (2), 372–384.
Weers, J.G., Miller, D.P., 2015. Formulation design of dry powders for inhalation. J. Pharm. Sci. 104 (10), 3259–3288.
Young, P., Cocconi, D., Colombo, P., Bettini, R., Price, R., Steele, D., Tobyn, M., 2002. Characterization of a surface modified dry powder inhalation carrier prepared by "particle smoothing". J. Pharm. Pharmacol. 54 (10), 1339–1344.
Yu, J., Chan, H.-K., Gengenbach, T., Denman, J.A., 2017. Protection of hydrophobic amino acids against moisture-induced deterioration in the aerosolization performance of highly hygroscopic spray-dried powders. Eur. J. Pharm. Biopharm.
Zhou, Q.T., Qu, L., Larson, I., Stewart, P.J., Morton, D.A., 2010. Improving aerosolization of drug powders by reducing powder intrinsic cohesion via a mechanical dry coating approach. Int. J. Pharm. 394 (1), 50–59.
Zhou, Q.T., Denman, J.A., Gengenbach, T., Das, S., Qu, L., Zhang, H., Larson, I., Stewart, P.J., Morton, D.A., 2011a. Characterization of the surface properties of a model pharmaceutical fine powder modified with a pharmaceutical lubricant to improve flow via a mechanical dry coating approach. J. Pharm. Sci. 100 (8), 3421–3430.
Zhou, Q.T., Qu, L., Gengenbach, T., Denman, J.A., Larson, I., Stewart, P.J., Morton, D.A., 2011b. Investigation of the extent of surface coating via mechanofusion with varying additive levels and the influences on bulk powder flow properties. Int. J. Pharm. 413 (1), 36–43.
Zhou, Q.T., Qu, L., Gengenbach, T., Larson, I., Stewart, P.J., Morton, D.A., 2013. Effect of surface coating with magnesium stearate via mechanical dry powder coating approach on the aerosol performance of micronized drug powders from dry powder inhalers. AAPS PharmSciTech 14 (1), 38–44.
Zhou, Q.T., Gengenbach, T., Denman, J.A., Heidi, H.Y., Li, J., Chan, H.K., 2014. Synergistic antibiotic combination powders of colistin and rifampicin provide high aerosolization efficiency and moisture protection. AAPS J. 16 (1), 37–47.
Zhou, Q.T., Loh, Z.H., Yu, J., Sun, S.-P., Gengenbach, T., Denman, J.A., Li, J., Chan, H.-K., 2016. How much surface coating of hydrophobic azithromycin is sufficient to prevent moisture-induced decrease in aerosolisation of hygroscopic amorphous colistin powder? AAPS J. 1–12.
Zhu, K., Tan, R.B., Ng, W.K., Shen, S., Zhou, Q., Heng, P.W., 2008. Analysis of the influence of relative humidity on the moisture sorption of particles and the aerosolization process in a dry powder inhaler. J. Aerosol Sci. 39 (6), 510–524.